ENVIRONMENTAL ENGINEERING SCIENCE
Volume 00, Number 00, 2025

DOI: 10.1089/ees.2024.0358

Organic Matter Removal of Biogas-Digested Pig Wastewater Using an Upflow Anaerobic Biochar-Based Filter Column

T. Phuong Nguyen,[1] T.C. Phuong Tran,[1] T.T. Nguyen Nguyen,[1] Thang P. Nguyen,[2] Quyet V. Le,[3] N-Thanh Nguyen,[4,5] and X. Cuong Nguyen[4,5,*]

[1]*Faculty of Environmental Engineering Technology, Hue University, Hue City, Vietnam.*
[2]*Department of Chemical and Biological Engineering, Gachon University, Seongnam-si, Republic of Korea.*
[3]*Department of Materials Science and Engineering, Korea University, Seoul, Republic of Korea.*
[4]*Institute of Research and Development, Duy Tan University, Da Nang, Vietnam.*
[5]*Faculty of Environmental Chemical Engineering, Duy Tan University, Da Nang, Vietnam.*

Received: November 30, 2024 *Accepted in revised form: March 28, 2025*

Abstract

This study evaluates the performance of an upflow anaerobic biochar-based filter column for treating pig farm wastewater, addressing the limited application of biochar in this context. Biochar derived from *Mimosa pigra*, an invasive plant species, was utilized to explore its potential as a sustainable, cost-effective treatment medium. Two systems with varying hydraulic loading rates (HLR) and organic loading rates (OLR) were evaluated. Both systems achieved high chemical oxygen demand (COD) removal efficiency, ranging from 84.90% to 85.62% within the first 12 days. The system operating under higher OLR and HLR exhibited slightly better COD removal efficiency (78.22 ± 5.05%) compared with the lower-rate system (77.93 ± 5.44%). The results suggest that increased OLR generally enhances COD removal, while higher HLR may reduce efficiency by decreasing biofilter contact time. Despite elevated HLRs, effluent COD remained within discharge limits, indicating the potential to optimize HLR and OLR for improved performance and cost-efficiency. This study provides new insights into the application of invasive plant-derived biochar in pig farm wastewater treatment, contributing to more sustainable waste management practices.

Keywords: anaerobic filter; biochar; COD removal; hydraulic loading rate; organic loading rate; pig wastewater

Introduction

Managing livestock waste on farms is challenging, particularly for small-scale farms in developing countries (Phan et al., 2022). Swine wastewater is rich in solids, organic matter, and nutrients, depleting dissolved oxygen and endangering aquatic ecosystems and human health (Gaur et al., 2022). Anaerobic digestion is commonly used to reduce pollutant concentrations and produce biogas in livestock wastewater treatment (Lourinho et al., 2020; Zhou et al., 2024). Despite anaerobic treatment, swine wastewater still contains high contaminants, failing to meet environmental standards (Pu et al., 2022). While some farms use bio- or fishponds for further treatment, this is only feasible for those with larger land areas (Nguyen et al., 2021). Thus, a cost-effective solution is needed to reduce pollution from swine effluent, particularly for small-scale farms and households.

Biofilter technology is considered to have a simple operation, low energy requirement, environmental friendliness, and low wastewater treatment costs (Terán et al., 2017). It was used for remediating swine wastewater (Escalante-Estrada et al., 2019; Zhao et al., 2020). The filter material is crucial in biofilter systems, as it affects effluent wastewater quality by providing a surface area for microorganisms to attach and grow (Zhao et al., 2020). Different types of materials in biofilters were employed for swine wastewater treatment, such as utilized gravel, soil, woodchips (Zhao et al., 2020), activated carbon, zeolite, Pall rings (Forbis-Stokes et al., 2018), and red volcanic rock (Terán et al., 2017). Biofilters, while effective, are less competitive than aerobic bioprocesses due to their large footprint, especially with traditional materials like sand and gravel (Marycz, 2023). These materials also suffer from clogging and long start-up periods, requiring frequent maintenance (Dobslaw et al., 2018;

**Corresponding author:* Institute of Research and Development, Duy Tan University, 03 Quang Trung, Da Nang 550000, Vietnam. *E-mail:* nguyenxuancuong4@duytan.edu.vn

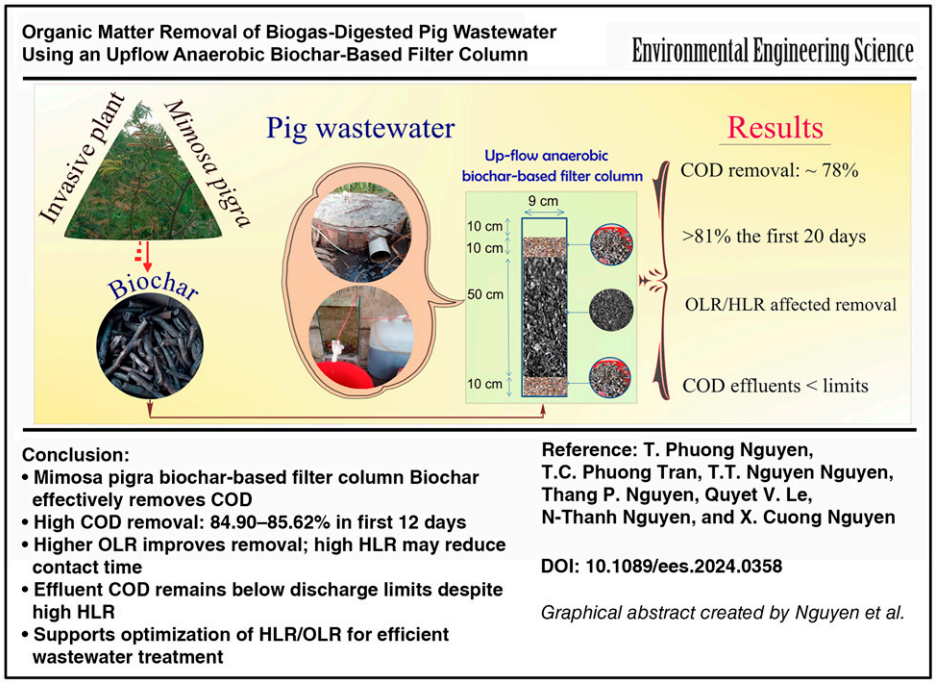

Loh et al., 2021; Mohamed et al., 2023). Therefore, recent studies have focused on developing new filter materials to minimize clogging, enhance treatment efficiency, and reduce costs.

Biochar has gained attention as a cost-effective and practical material for constructed wetlands and biofilter systems due to its exceptional contaminant adsorption capacity, driven by its high surface area, porosity, and functional groups (Almanassra et al., 2021; Nguyen et al., 2020). It efficiently adsorbs various pollutants, including organic and inorganic substances, nutrients, heavy metals, and pathogens (Almanassra et al., 2021; Truong et al., 2023). The pyrolysis process, including temperature, heating rate, and residence time, directly impacts biochar's physicochemical properties (Xiang et al., 2020; Yaashikaa et al., 2020). Higher production temperatures typically increase surface area and porosity (Bui et al., 2024; Tomczyk et al., 2020), enhancing cation exchange capacity and adsorption performance (Leng et al., 2021). Biochar with greater surface area and porosity also promotes biofilm development, improving filtration efficiency (Dalahmeh, 2016; Yaashikaa et al., 2020). Its high porosity allows better water retention and supports biofilm growth without clogging, outperforming less porous materials (Fajar et al., 2022). Additionally, functional groups such as C = O, –OH, $–CH_2$, and COOH, influenced by feedstock and production temperature, determine biochar's ability to adsorb organic and inorganic compounds (Enaime et al., 2020; Li et al., 2017; Li et al., 2023).

While biochar-based biofilters have effectively treated various effluents, including domestic, livestock, and industrial wastewater, research specifically targeting swine wastewater treatment remains limited (Jayabalakrishnan et al., 2024; Kaetzl et al., 2018; Kaetzl et al., 2019). Existing studies primarily focus on domestic wastewater treatment or specific types of industrial effluents, with limited attention given to the challenges posed by agricultural wastewater, mainly from pig farms. No studies have used *Mimosa pigra* biochar filters to treat pig farm wastewater.

This study introduces an innovative approach using biochar derived from the invasive *M. pigra* in upflow anaerobic filters (UAF) for small-scale pig farms. Unlike prior studies on generic biochar applications for domestic or industrial effluents, this research addresses the often-overlooked issue of swine wastewater treatment, a major source of agricultural pollution. The choice of *M. pigra*–based biochar is grounded in its dual environmental and functional advantages: repurposing an invasive species into a sustainable, cost-effective feedstock while leveraging its proven adsorption properties—high surface area and porosity—as shown in previous studies (Nguyen, 2021; Phuong Tran et al., 2021; Tran et al., 2022). Despite these promising properties, its application for swine wastewater remains underexplored, making this study a novel contribution. Further, by examining the impact of hydraulic loading rates (HLR) and organic loading rates (OLR) on treatment performance, this work offers practical insights for real-world pig farm operations, advancing knowledge on agricultural wastewater management beyond existing literature.

Materials and Methods

Wastewater

Swine wastewater was collected from a biogas tank outlet for household pig production in Hai Lang district, Quang Tri province, Vietnam. The raw effluent was purified through a sand tank filter to remove suspended solids. The wastewater was then stored in a plastic container in a fridge and renewed twice a week. The average chemical oxygen demand (COD) concentration of the wastewater after passing through the sand filter across all preparation batches was $\sim$753.43 $\pm$ 94.58 mg/L (n = 24). COD was analyzed using SMEWW

5220 D (APHA, 2017). The COD concentration in this study was comparable with that reported in other studies: 660 mg/L (Thai et al., 2022), 505.3 ± 706.9 mg/L (Nguyen et al., 2021), and 701.76 ± 33.21 mg/L (Huong, 2023). Depending on the stage of the study, the wastewater was either diluted twice or thrice with tap water or not diluted.

Filter material

Preparation. The primary filter material used in the experiment was biochar derived from the *M. pigra* plant. *Mimosa* trees were collected locally, with the shells and leaves removed. The stalks were dried outdoors for 3 days to reduce humidity and then cut into 7–8 cm pieces. These pieces were placed in closed tin boxes to limit oxygen exposure during pyrolysis. The boxes were placed in a self-produced oven with additional firewood around and on top. The fire was ignited at the bottom of the furnace, and the lid was closed. The temperature in the furnace is around 600°C. The pyrolysis process lasted ∼2 h. After cooling to room temperature, the biochar was removed from the boxes, crushed into small pieces (1–5 mm), and sieved over a 1 mm sieve to remove fine particles. The biochar production process from *M. pigra* plant is described in Figure 1. The biochar was washed with tap water three times to remove ashes and then stored in a basket for about 1 h before being used in the filter columns.

This study determined the physical properties of biochar, including water content, bulk density, particle density, and total porosity.

- The water content was determined by applying the formula (Eq. 1):

$$w = \frac{M_w}{M_s}, \tag{1}$$

where w is gravimetric water content (g/g), M_w is the mass of water (g), and M_s is the mass of solids (g). The air-dried biochar was put in a furnace at 105°C for 24 h. The mass of water was determined as the weight of the air-dried biochar minus the weight of the oven-dried biochar.

- The bulk density reflects the mass or weight of a given volume. It includes the volume occupied by solid particles and the voids (pores, cracks, etc.) between them. The bulk density is the dry biochar media weight divided by the volume occupied by the media (Eq. 2).

$$\rho = \frac{M_s}{V_s} \tag{2}$$

where ρ is the bulk density (g/cm^3), M_s is the dry biochar media weight (g), and V_s is the volume occupied by the media (cm^3).

Particle density refers to the mass per unit volume of the solid particles, excluding the void spaces between them. This was assessed using the liquid immersion technique, where the volume of deionized water displaced by the particles was measured. Air-filled pores were eliminated by gently boiling the mixture. The submerged particles were then allowed to saturate for 24 h.

The particle density of the biochar was determined by applying the formula (Eq. 3):

$$\rho_s = \frac{M_s}{V_s}, \tag{3}$$

where ρ_s is the particle density (g/cm^3), M_s is the mass of biochar (g), and V_s is the volume of biochar (cm^3).

The porosity of biochar was based on the particle density and bulk density of biochar using the formula (Eq. 4):

$$f = 1 - \frac{\rho}{\rho_s} \times 100, \tag{4}$$

where f is the total porosity (%), ρ is the bulk density (g/cm^3), and ρ_s is the particle density (g/cm^3).

UAF design and operation. Our study introduced two novel UAF systems, each designed with unique features.

FIG. 1. Biochar production process: **(a)** *Mimosa* trees, an invasive species, used as the raw material; **(b)** shell and leaf removal, followed by drying and cutting into 7–8 cm pieces; **(c)** furnace operation and biochar formation after 2 h of pyrolysis; and **(d)** final biochar product with a particle size of ∼1–5 mm.

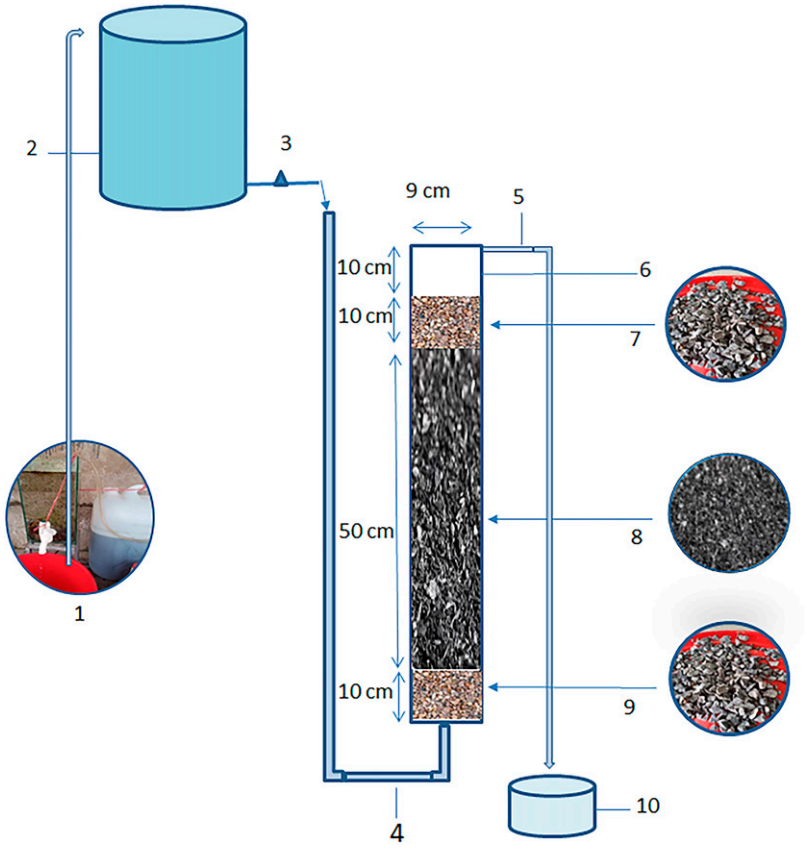

FIG. 2. Schematic diagram of the biochar-based filter column: **(1)** Raw wastewater filtered through the sand filter, **(2)** reservoir, **(3)** flow control, **(4)** anaerobic influent, **(5)** anaerobic effluent, **(6)** supernatant water layer, **(7)** top gravel layer, **(8)** biochar media, **(9)** bottom gravel layer, and **(10)** sampling point.

The systems, identical in design, were constructed using polyvinyl chloride (PVC) filter columns, each with a total height of 80 cm and a diameter of 9 cm (Fig. 2). The effective volume of each column was 3.2 L, filled with the filter materials. One system operated with diluted wastewater (system A), while the other operated with raw sewage (system B). Both UAFs were operated simultaneously under the same environmental conditions. This experimental design aimed to evaluate the behavior of UAF systems under different COD and loading strengths. Each UAF column was filled with three layers: a 10 cm layer of gravel (1–2 cm diameter) at the bottom, a primary layer of 50 cm of biochar (added in 10 cm increments and lightly pressed), a 10 cm gravel layer at the top, and a 10 cm supernatant water layer. The outlet valve was positioned just above the supernatant water layer. A 10 L wastewater reservoir, positioned 1.5 m above ground, enabled a gravity-driven flow into the UAF. Wastewater exited the reservoir through a bottom valve into a 1.4 m long, 3 cm diameter PVC tube, directing flow to the UAF column's base, ensuring an upward flow through the system. The 1.4 m inlet pipe minimized oxygen diffusion from the influent, while the 10 cm supernatant water layer at the outlet further restricted oxygen ingress. The system design maintained predominantly anaerobic conditions with no forced aeration or mixing.

Our experimental design was comprehensive, aiming to cover all aspects of UAF performance. Initially, the UAF was continuously operated with tap water at 10 mL/min for 2 days to control flow, HLR, and hydraulic retention time. After that, natural wastewater was loaded into the UAF in an upflow, saturated, and intermittent regime. The inlet was fed thrice daily at 6 a.m., 11 a.m., and 5 p.m. The wastewater-fed mode imitated the wastewater discharge when barn cleaning at household pig farms. The total time wastewater was fed was 60 min per time. Depending on the stages of the experiments, the wastewater-fed loading rates were 5, 10, and 15 mL/min. The current study tested the performance of UAFs at three HLR regimes and three levels of COD influent concentration.

Sampling and analyses. The samples were collected at two crucial locations: the inflow and outflow of UAFs, one every 2 days at 6:30 a.m. These samples were immediately analyzed, ensuring the utmost accuracy. We tested for COD according to SMEWW 5220 D (APHA, 2017), and each sample was analyzed in triplicate to confirm our findings.

The OLR and HLR were calculated according to the following formulas (Eqs. 5 and 6):

$$\mathrm{OLR} = \frac{Q.C_{\mathrm{in}}}{V}\left(\mathrm{g/m^3{\cdot}d}\right) \tag{5}$$

$$\mathrm{HLR} = \frac{Q}{\mathrm{A}}\left(\mathrm{m/d}\right) \tag{6}$$

where Q is the wastewater flow (m^3/d), C_{in} is the influent COD concentration (mg/L), V is the helpful volume of the

treatment tank (m^3), and A is the cross-sectional area of the filter column (m^2).

The efficiency in the reduction of COD was calculated with the following formula (Eq. 7):

$$E = \frac{C_{in} - C_{eff}}{C_{in}} .100\% \quad (7)$$

where C_{in} is the influent COD concentration (mg/L), and C_{eff} is the effluent COD concentration (mg/L).

To evaluate the differences in treatment efficiency, we used a one-way analysis of variance (ANOVA) at a 95% confidence level. This analysis helps to determine whether there are significant differences between groups with different OLR and HLR values. The data were tested for homogeneity of variance before performing ANOVA. The ANOVA test was conducted using IBM SPSS Statistics v25.0 software. A 95% confidence level was set, meaning a p value <0.05 was considered statistically significant for differences between groups. If the ANOVA results showed significant differences, multiple comparisons of Tukey's HSD would be performed to identify which groups differ significantly.

Each HLR or OLR group was operated for 34 days in stage I, 18 days in stages II and IV, and 16 days in stage III, with samples collected every 2 days. Consequently, each group had 17 repetitions in stage I, 9 in stages II and IV, and 8 in stage III. For the ANOVA analysis, the performance of each repetition was represented by the mean of three replicate measurements per sample.

Analysis of biochar properties. Our study employed advanced analytical techniques to assess the properties of biochar. A survey assessed the presence of functional groups on biochar before and after adsorption using a Fourier-transform infrared (FTIR) spectrometer, covering the range of 4000–500/cm with a resolution of 2/cm. Elemental composition and surface percentages of common elements were determined using the Thermo Scientific K-Alpha X-ray Photoelectron Spectrometer, with spectra analyzed in standard lens mode at pass energy of 200 eV, spanning 0–1200 eV with a 1 eV energy step. Surface area measurements were conducted as multipoint Brunauer–Emmet–Teller (BET) from N_2 adsorption isotherms at 77.485 K using ASAP 2020 V3.00 H. The scanning electron microscope (SEM) images were obtained using the SEM Hitachi SU8600 (Hitachi High-Tech Corporation).

Results and Discussion

Physical properties of biochar

The physical characteristics of biochar include water content, bulk and particle density, and porosity. The water content of the biochar was 5.92%, indicating a relatively low moisture level. The bulk density was measured at 148.45 g/cm^3, while the particle density was significantly higher at 478 g/cm^3. The total porosity of the biochar was 31.05%, suggesting a substantially porous structure. This enables biochar filters to retain water better in the pores while facilitating the development of biofilms, which serve as habitats for microorganisms to absorb and degrade pollutants in the water (Dalahmeh, 2016).

The results of biochar surface properties show a high BET surface area of 172.71 m^2/g and a Langmuir surface area of 229.91 m^2/g, along with a significant t-Plot micropore volume of 0.059 cm^3/g (Supplementary Table S1). Moreover, the moderate average pore widths (4.97 nm for Barrett–Joyner–Halenda [BJH] adsorption and 4.54 nm for BJH desorption) illustrate that *Mimosa* biochar has a highly porous structure with a large surface area, which is favorable for adsorption applications. Biochar surface areas and total pore volumes typically range from 8 to 132 m^2/g and 0.016 to 0.083 cm^3/g, but they can reach as high as 490.8 m^2/g and 0.25 cm^3/g,

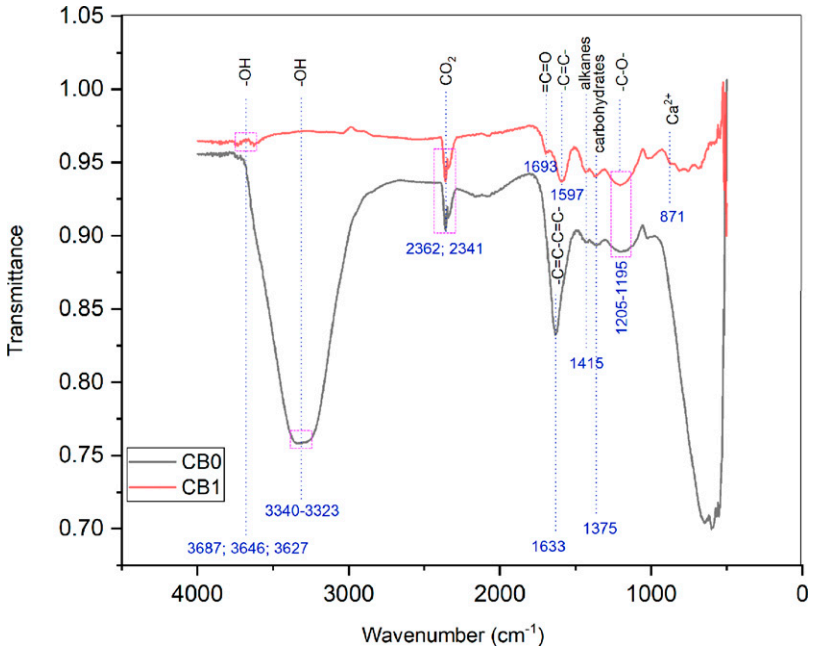

FIG. 3. FTIR spectrum of biochar before and after adsorption: CB0 presents biochar before adsorption and CB1 presents biochar after adsorption.

respectively (Leng et al., 2021). For example, the BET surface area of biochar from date palms varies from 2.04 to 249.13 m^2/g, with pore volumes ranging from 0.006 to 0.031 cm^3/g (Elnour et al., 2019). Chowdhury et al. (2016) reported a significant increase in the BET surface area of wood sawdust biochar, from 2.567 to 220.989 m^2/g, and in pore volume from 0.005 to 0.009 cm^3/g, as the pyrolysis temperature rose from 350°C to 550°C. These comparisons suggest that the biochar in our study exhibits notable surface properties, providing numerous sites for adsorption both on its surface and within its pore structure. After the experiment, the postadsorption biochar samples were analyzed for surface area, revealing a drastic reduction in the BET surface area to 3.95 m^2/g and the Langmuir surface area to 5.44 m^2/g. This indicates that the adsorption capacity has been significantly utilized, with pollutants occupying the most available sites. The sharp decrease in t-Plot micropore volume to 0.0005 cm^3/g after adsorption highlights that the smallest pores have been filled, crucial for trapping small pollutant molecules. Additionally, the significant reduction in the micropore volume of biochar was also due to the development of biofilm covering the material's surface, including the biochar's macropores (Kaetzl et al., 2020).

Chemical and surface properties of biochar

The FTIR spectrum analysis (Fig. 3) illustrates that peaks at wavenumbers 3687, 3646, and 3627/cm, within the stretching region of 3700–3575/cm, indicate the presence of the –OH group (Dai et al., 2023; Mesto et al., 2012) within biochar after adsorption (CB1). In contrast, the biochar before adsorption (CB0) peaks in the 3340–3323/cm region, indicating –O–H stretching (Subratti et al., 2021). –OH groups enhance metal adsorption due to their hydrogen bonding capabilities and higher electronegativity compared with other functional groups, allowing them to complex more effectively with metal ions. Additionally, the oxidized functional groups on the biochar surface notably increase its hydrophilicity (Li et al., 2023), enabling better interaction with polar or water-soluble substances, such as metal ions, ammonium, or certain organic compounds. Both biochar samples also exhibit peaks at 2362–2341/cm, indicating the presence of CO_2 groups. This is attributed to the functional groups on biochar that can adsorb CO_2, with the gas retained on its surface (Dissanayake et al., 2020; Zhang et al., 2023) or possibly due to residual gases trapped during the biochar production process (Phuong Tran et al., 2021).

In CB1, the peak at 1693/cm indicates carbonyl bond (=C=O) stretching within ketones or carboxylic groups (Kim et al., 2021; Smith, 2017), while the peak at 1597/cm reflects the stretching vibrations of the double bond –C=C– in open-chain or branched structures (Elnour et al., 2019). Within the 1300–1000/cm range, two bands typically indicate the presence of the –C–O– bond in alcohols or ethers (Wahyono et al., 2019). In both CB0 and CB1, broad peaks in the 1205–1195/cm range indicate the presence of alcohols or ethers in these samples. These functional groups, including –C–O– and alcohol (–OH), play a crucial role in enhancing ammonium adsorption due to their high reactivity and ability to form hydrogen bonds (Yaashikaa et al., 2020).

In CB1, the peak at 871/cm demonstrates the presence of Ca^{2+} adsorbed (Delcourt et al., 2019) from wastewater

Table 1. Operating Parameters in Two Treatment Systems

	System A				*System B*			
Systems	*Stage I*	*Stage II*	*Stage III*	*Stage IV*	*Stage I*	*Stage II*	*Stage III*	*Stage IV*
Influent COD (mg/L)	159–400	186–328	437–636	174–329	159–400	539–833	550–857	589–858
Q (L/d)	0.9	1.8	1.8	2.7	0.9	0.9	1.8	2.7
HRT (d)	3.56	1.78	1.78	1.18	3.56	3.56	1.78	1.18
HLR (m/d)	0.142	0.283	0.283	0.425	0.142	0.142	0.283	0.425
OLR (g COD/[m3·d])	44.72–112.50	104.63–184.50	245.81–357.75	146.81–277.59	44.72–112.53	151.59–234.28	309.38–482.06	496.97–723.94
Operation period (d)	34	18	16	18	34	18	16	18

System A operated with diluted wastewater, while system B used raw wastewater, with dilution applied only in stage I. Stages II, III, and IV remained undiluted.
HLR, hydraulic loading rate; HRT, hydraulic retention time; OLR, organic loading rate; Q, inflow rate.

Table 2. Average Inflow COD (Chemical Oxygen Demand) Load and Removal Efficiency in Two Treatment Systems

	System A				*System B*			
	Stage I	*Stage II*	*Stage III*	*Stage IV*	*Stage I*	*Stage II*	*Stage III*	*Stage IV*
Influent COD (mg/L)	261 ± 71	258 ± 50	531 ± 78	280 ± 67	261 ± 71	743 ± 98	758 ± 108	760 ± 89
Effluent COD (mg/L)	47 ± 8	61 ± 13	115 ± 13	70 ± 10	53 ± 13	130 ± 17	171 ± 18	198 ± 31
OLR (g COD/[m^3·d])	73.37 ± 19.87	144.94 ± 28.25	298.90 ± 42.53	235.31 ± 52.78	73.37 ± 19.87	209.03 ± 27.68	426.09 ± 60.50	641.16 ± 75.12
COD removal (%)	80.87 ± 6.75	76.11 ± 3.50	78.14 ± 2.44	74.32 ± 3.60	78.92 ± 5.65	82.31 ± 3.13	77.19 ± 2.67	73.79 ± 3.45

System A operated with diluted wastewater, while system B used raw wastewater, with dilution applied only in stage I. Stages II, III, and IV remained undiluted.
HLR, hydraulic loading rate; HRT, hydraulic retention time; OLR, organic loading rate; Q, inflow rate.

during the treatment. The elemental composition analysis of the biochar surface before and after adsorption, shown in Supplementary Figure S1 a and b, reveals that CB1 shares common elements with CB0, such as O, N, C, and Cl. Also, CB1 shows the presence of Ca and P, with an increased N content compared with CB0. This suggests that the biochar effectively adsorbed N, P, and Ca-containing compounds. The significant changes in C and O content also indicate the biochar's effective adsorption of organic compounds.

Removal capacity

Two UAF systems, A and B, were operated with different operating parameters. Each system was divided into four stages, each running under distinct conditions. The operating parameters for both systems throughout the experiment are presented in Table 1.

COD removal under different loadings. Experiments were conducted under different COD load conditions to evaluate their impacts on the treatment efficiency of the UAFs. In system A, the wastewater was diluted thrice during stages (I, II, and IV) and twice during stage III. In system B, the wastewater remained undiluted in the final three stages (II, III, and IV). Depending on the changes in the inflow rate and the initial wastewater concentration, the organic load into the system varied across different stages (Table 2).

When the influent COD concentration increased from 258 ± 50 mg/L (phase II) to 531 ± 76 mg/L (phase III), the OLR rose from 144.94 ± 28.25 to 298.90 ± 42.53 g COD/(m^3·d), resulting in a slight increase in COD removal efficiency from 76.11 ± 3.50% to 78.14 ± 2.44% in system A. However, when the influent COD concentration and OLR decreased in phase IV (235.31 ± 52.78 g COD/[m^3·d]), the COD removal efficiency dropped to 74.32 ± 3.60% (Fig. 4). A similar trend was observed in system B. When the OLR increased from 73.37 ± 19.87 g COD/(m^3·d) (stage I) to 209.03 ± 27.68 g COD/(m^3·d) (stage II), the COD removal efficiency improved from 78.92 ± 5.65% to 82.31 ± 3.13%. However, as OLR continued to rise in stage III (426.09 ± 60.50 g COD/[m^3·d]) and IV (641.16 ± 75.12 g COD/[m^3·d]), COD removal efficiency declined to 77.19 ± 2.67% and 73.79 ± 3.45%, respectively (Fig. 5). The reduced efficiency in stages III and IV coincided with increased HLR, which shortened contact time and impacted COD removal performance.

ANOVA analysis showed that changes in OLR significantly affected COD removal rates ($p < 0.05$ for both systems A and B). However, the *post hoc* test results indicated that significant differences in COD removal efficiency ($p < 0.05$) occurred between the OLR values of 73.37 and 235.31 g COD/(m^3·d) in system A (stages I and IV), and between 73.37 and 641.16 g COD/(m^3·d) (stages I and IV), as well as between 209.03 and 641.16 g COD/(m^3 d) (stages II and IV) in system B. Changes in OLR during the other stages did not significantly affect COD removal efficiency ($p > 0.05$). This is likely due to the system reaching a performance plateau, where microbial adaptation and biofilm development stabilized COD removal across specific OLR ranges. Additionally, the overlapping influence of HLR, especially in stages III and IV of system B, reduced the contact time between wastewater and the biofilm, partially offsetting the impact of increased

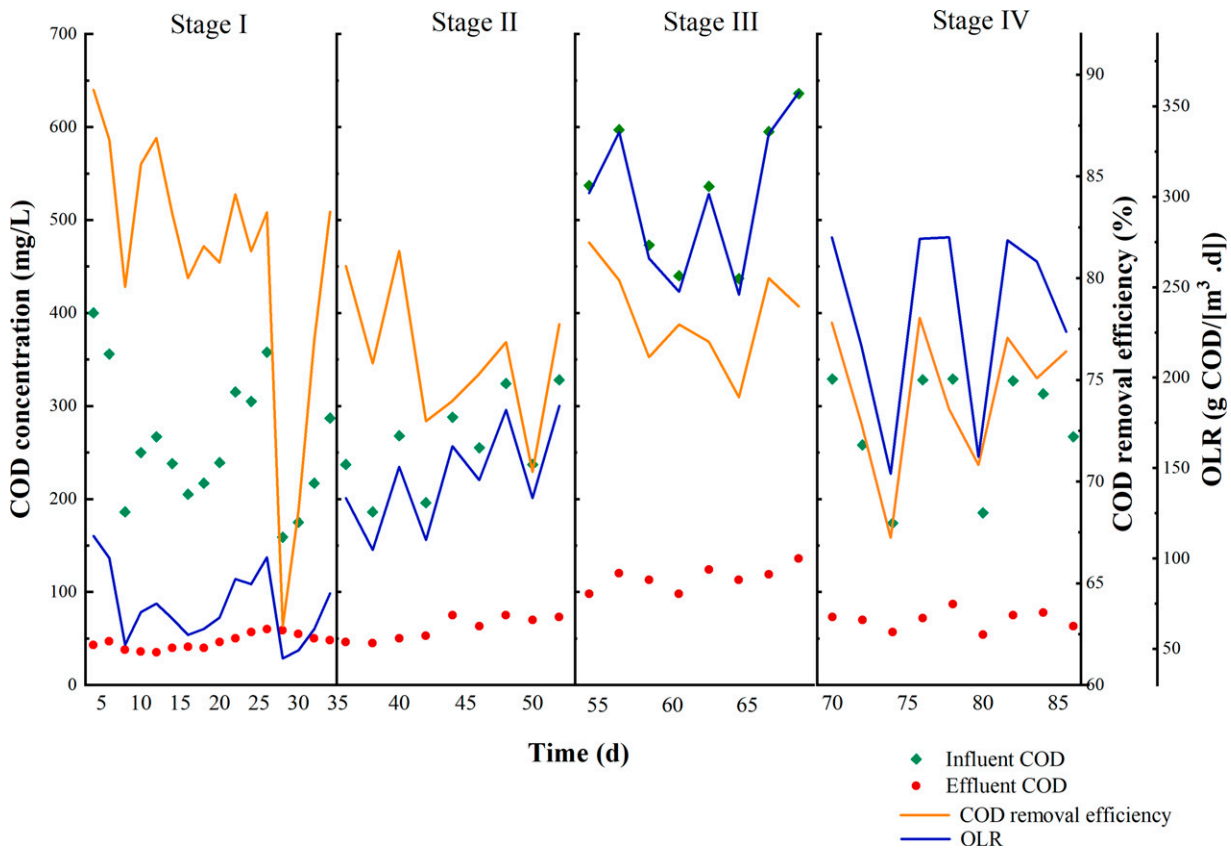

FIG. 4. Chemical oxygen demand (COD) concentration, removal rate, and organic loading rate (OLR) across different stages in system A (upflow anaerobic filter operated with diluted wastewater).

OLR. Furthermore, at higher OLRs (stages III and IV), biochar adsorption sites may have reached saturation, making biodegradation the primary removal mechanism, which responds more gradually to changes in loading rates. In the study by Perez-Mercado et al. (2018), operating spruce-biochar filters at different OLR conditions (5 ± 2 and 20 ± 5 g BOD_5/[m^2 d]) did not significantly impact COD removal efficiency. However, the efficiency at OLR 20 ± 5 g BOD_5/(m^2 d) (99%) was higher than at 5 ± 2 g BOD_5/(m^2 d) (95%). Biochar filters showed a solid ability to stabilize variations in loading conditions, as demonstrated by their ability to maintain high COD removal rates with an average fluctuation of around 25% in organic load (Perez-Mercado et al., 2018). These results suggest that while OLR can significantly affect COD removal rates, this effect is dependent on specific conditions. This can be observed in the treatment systems when increasing the OLR from stage II to III, as system A's COD removal efficiency changed insignificantly (~2%). This limited variation suggests that the system may have reached its optimal COD removal capacity. Despite the higher influent COD concentration, the treatment efficiency remained stable, possibly due to the biochar filter reaching its maximum adsorption capacity, with adsorption sites nearing saturation. Also, COD removal efficiency is influenced by multiple factors beyond OLR, such as water flow rate, filter structure, biochar properties, and microbial growth and activity. These combined factors can limit variations in efficiency, even under increased organic loading.

Effect of HLRs on COD removal. The HLR parameters in the experiments were adjusted by changing the influent wastewater flow rate. The experiments examined COD treatment efficiency at three HLR values corresponding to different OLRs (Table 1). Figure 6 illustrates the effect of HLRs on the COD removal performance of UAFs.

In system A, when the HLR increased from 0.142 (stage I) to 0.283 m/d (stage II), the COD removal efficiency dropped from 80.87 ± 6.75% to 76.11 ± 3.50%. A similar trend was observed in stage IV, where the HLR further increased to 0.425 m/d (HRT reduced to 1.18 days), and the COD removal rate decreased to 74.32 ± 3.60%. In system B, a decrease in COD removal performance was noted in stage III, where the efficiency dropped to 78.14 ± 2.44%, despite the influent COD concentration being similar to stage II. This reduction is likely due to the increased HLR in stage III (0.283 m/d). The trend continued in stage IV, where the HLR increased to 0.425 m/d, decreasing efficiency to 74.32 ± 3.60%. These results suggest that as HLR increases, COD removal efficiency decreases, consistent with findings reported by Rehman et al. (2019).

The ANOVA analysis results show that HLR significantly affects COD removal efficiency ($p = 0.008$ in system A and $p = 0.002$ in system B). While significant changes in HLR, such as from 0.142 to 0.425 m/d, had a notable impact on COD removal rates ($p < 0.05$), more minor changes in HLR (from 0.142 to 0.283 m/d and from 0.283 to 0.425 m/d) did not significantly affect COD removal

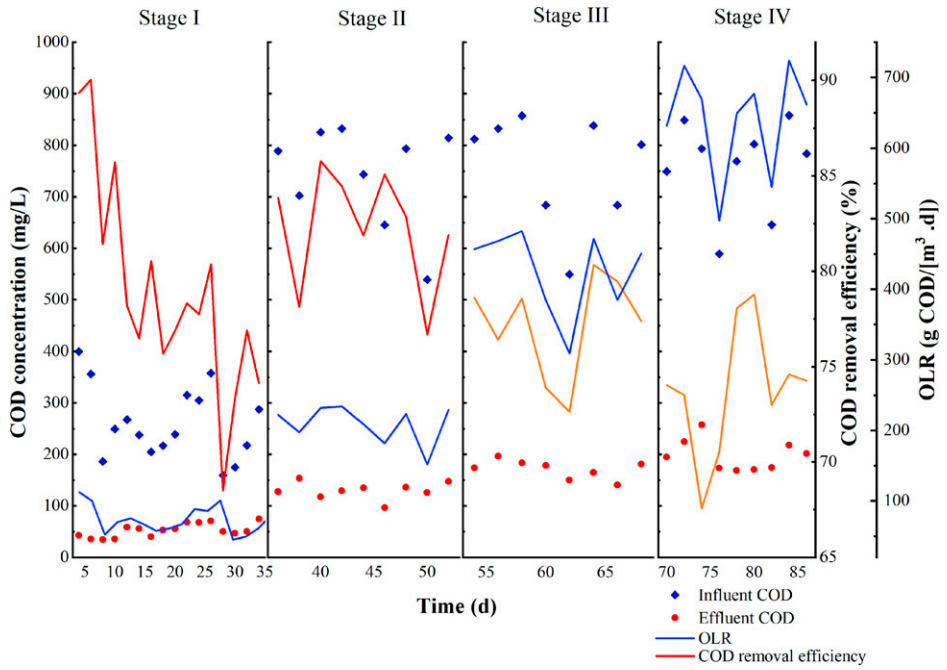

FIG. 5. Chemical oxygen demand (COD) concentration, removal rate, and organic loading rate (OLR) across different stages in system B (upflow anaerobic filter operated with raw sewage).

rates ($p > 0.05$). Some studies have also reported that HLR did not significantly increase COD removal rates. For instance, Perez-Mercado et al. (2018) reported COD removal ranging from 94% to 99% at both tested HLRs (0.034 and 0.2 m/d). Similarly, Dalahmeh et al. (2019b) found that changing the HLR from 0.023 to 0.039 m/d did not affect COD reduction, with overall efficiency remaining between 90% and 93% across different HLRs ($p > 0.05$).

Discussion

Figures 4–6 show that the UAF system achieved high COD removal efficiency from the start, exceeding 85.62% in system A and 84.90% in system B within the first 12 days. During this period, the removal efficiency peaked but subsequently decreased and became unstable for the remainder of stage I. The biochar filter exhibited effective COD removal from the start of the treatment process, primarily due to

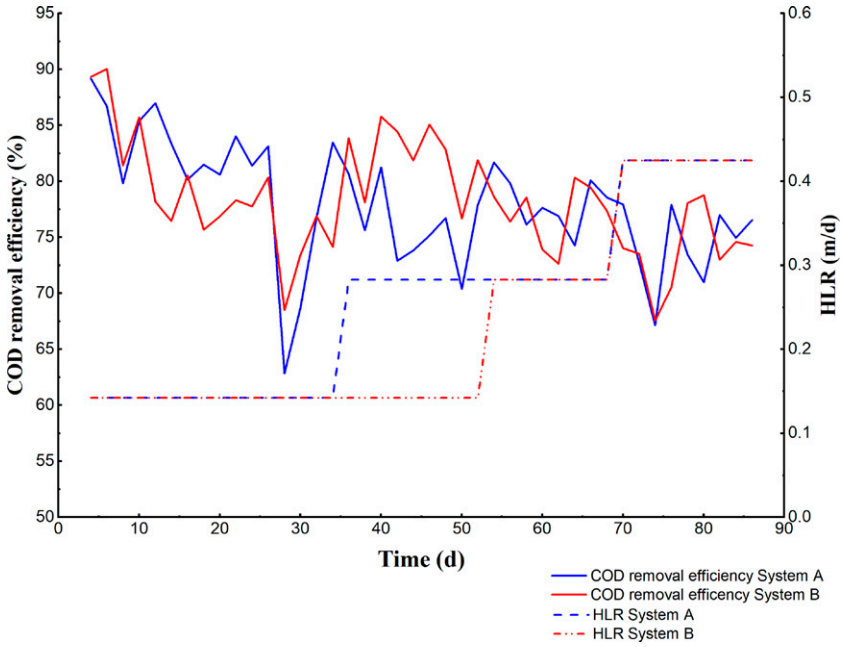

FIG. 6. Hydraulic loading rate (HLR) and chemical oxygen demand (COD) removal rates across different stages in system A (diluted wastewater) and system B (raw sewage) in upflow anaerobic filters.

pollutant adsorption onto the biochar surface, as biofilm formation had not yet occurred. In contrast, conventional biological filtration systems typically require 3–60 days for microorganisms to develop biofilms and achieve optimal treatment efficiency (Dalahmeh, 2016). This was indicated in the study by Dalahmeh et al. (2019a), where the biochar filter achieved higher COD removal efficiency in the early stages compared with the sand filter. It was attributed to the larger surface area of biochar (184 m^2/g) compared with the significantly lower surface area of sand (0.153 m^2/g), which enhanced adsorption performance in the biochar filter. Studies confirm that biochar filters eliminate the need for prolonged warm-up periods, maintaining effective treatment from the start (Dalahmeh, 2016; Kaetzl et al., 2019; Song et al., 2024). In our current study, the COD removal efficiency on the 28th day of operation fell to its lowest point before rising again. This pattern is similar to findings from Kaetzl et al. (2020), where the COD removal efficiency of the biochar filter dropped from over 80% to 50% after 3 weeks. This decline was attributed to a decrease in the adsorption capacity of biochar, along with the release of excess biomass and degradation of organic particles. By the end of the experiment, COD removal efficiency increased and stabilized within the range of 65–75%, indicating a shift to biological decomposition as the primary removal mechanism. This improvement resulted from enhanced microbial activity within the biofilm, facilitating organic matter breakdown. Several studies have reported similar observations in biochar filter systems. SEM analysis at a depth of 10 cm confirmed extensive biofilm development, with the biofilm fully covering the filter material, including the porous structures of the biochar (Kaetzl et al., 2020). Adding biochar promoted biofilm formation and increased microbial community diversity, enhancing organic matter decomposition (Bui et al., 2024). The critical role of biofilms in COD removal has been demonstrated in previous studies. For example, Dalahmeh et al. (2018) demonstrated the crucial role of biofilms, as the COD removal efficiency in biochar-inactive-biofilm filters (61 ± 14%) was significantly lower ($p < 0.05$) compared with biochar-active-biofilm and sand-active-biofilm filters, which achieved an average COD removal rate of 94 ± 4%. This comparison highlights that biofilm activity is essential for maintaining stable and efficient COD removal.

The mean COD treatment performance during the stages was 77.93 ± 5.44% for system A and 78.22 ± 5.05% for system B. System A operated under HLR conditions ranging from 0.142 to 0.425 m/d (average 0.260 ± 0.108 m/d) and OLR conditions ranging from 44.72 to 357.75 g COD/(m^3 d) (average 166.37 ± 95.39 g COD/[m^3 d]). System B operated under HLR conditions ranging from 0.142 to 0.425 m/d (average 0.229 ± 0.117 m/d) and OLR conditions ranging from 44.72 to 723.94 g COD/(m^3 d) (average 291.29 ± 229.03 g COD/[m^2 d]). This performance surpasses that reported by Kaetzl et al. (2020) for *Miscanthus*-biochar anaerobic filters, which achieved a 74 ± 18% COD reduction in municipal wastewater but under higher OLR (509 g COD/[m^3 d]) and HLR (1.2 m/d) (Table 3). Dalahmeh (2016) observed over 90% COD removal with hardwood and willow biochar filters, though at lower HLR (0.034–0.199 m/d) and OLR (5–70 g BOD_5/[m^2 d]). Similarly, Perez-Mercado et al. (2018) reported COD removal of 94–99% in willow and pine-spruce biochar-based systems, also under lower HLR (0.031–0.199 m/d) and OLR (5–20 g BOD_5/[m^2·d]). Further, the COD reduction in digested swine wastewater reached 80.27% with the bamboo biochar filter column (Xin et al., 2021).

Table 3. The Effectiveness of COD (Chemical Oxygen Demand) Removal by Biochar Filters in Various Studies

Source of biomass	*Type of ww*	*Type of configuration*	*HLR ($m\ d^{-1}$)*	*OLR ($g\ COD\ m^{-3}d^{-1}$)*	*Efficiency of COD (%)*	*Ref.*
Pine-spruce, willow	Domestic	SBF	0.034	20 ± 5[a]	94–99	(Perez-Mercado et al., 2018)
Rice husk	Municipal ww	SBF	1.2	63 ± 16	52	(Kaetzl et al., 2019)
Mango peels	Real domestic	MMBF	0.24–0.319	—	97	(Majumder and Das, 2022)
Miscanthus grass	Real municipal ww	SBF	1.2	509 ± 173	74	(Kaetzl et al., 2020)
Birch, aspen, and alder wood chips	Ww from septic tank	MMBF	0.041	—	>60%	(Kholoma et al., 2020)
Coconut shells	Real textile dyeing ww	SBF	10.08	—	BOD: 57.5 COD: 86.8	(Jayabalakrishnan et al., 2024)
Mixture of pine and spruce wood biomass	Real domestic ww	SBF	0.023 0.031 0.038	—	90–93	(Dalahmeh et al., 2019b)
Soft woods	Real municipal ww	SBF	1.2	252	87	(Kaetzl et al., 2018)
Pine pellets	Ww from anaerobic digestion effluent	SBF	0.168	380	56	(Forbis-Stokes et al., 2018)
Bamboo biomass	Digested swine ww	SBF	—	—	80.27	(Xin et al., 2021)

[a]g COD/(m^2 d).
MMBF, multimedia biochar filter; Ref, reference; SBF, single biochar filter; ww, wastewater.

The results indicated that system B achieved a slightly higher average COD removal efficiency (78.22 ± 5.05%) than system A (77.93 ± 5.44%) despite operating under a higher OLR with undiluted COD concentrations. ANOVA analysis confirmed that OLR and HLR significantly influence COD treatment efficiency. Generally, higher OLR improved efficiency, as observed in system A, where increasing the OLR from stage II to stage III boosted COD removal. This improvement is attributed to enhanced biofilm growth and microbial activity, with a thicker biofilm layer increasing water retention and extending contact time for microbial degradation (Kaetzl et al., 2020). However, in system B, COD removal efficiency decreased when the OLR increased from stage II to stages III and IV, likely due to biochar adsorption site saturation and reduced efficiency (Dong et al., 2023). Excessive biofilm growth may also cause clogging and reduce efficiency through biofilm sloughing (Dalahmeh, 2016). In system B, both HLR and OLR increased simultaneously from stage II to stages III and IV. A higher HLR reduces treatment efficiency by shortening wastewater contact time and potentially washing out trapped organic matter and biofilm (Dalahmeh et al., 2014). Conversely, lower HLR (longer HRT) improved organic matter removal by extending contact time (Perez-Mercado et al., 2018).

Balanced OLR and HLR are essential for optimizing wastewater treatment efficiency while considering construction and operational costs. Finding the optimal values by evaluating their impact on processing efficiency can ensure high performance and economic feasibility, as high HLR reduces the system's volume, making it more cost-effective. In contrast, low HLR demands more space, which may be a constraint in area-limited regions (Kaetzl et al., 2020). In our study, operating with undiluted influent wastewater and an HLR of 0.142 m/d provided the highest treatment efficiency. As the HLR increased to 0.283 and 0.425 m/d, efficiency declined. On average, the COD concentration of pig farm wastewater in system B was 166 mg/L (185 mg/L under optimal conditions). While it meets livestock wastewater discharge standards (<300 mg/L for nondomestic water use, QCVN 62-MT:2016/BTNMT; MONRE, 2016), it exceeds the stricter limits for domestic discharges (50–110 mg/L for urban and concentrated residential areas, QCVN 14:2025/BTNMT; MONRE, 2025). These systems help pig farmers meet legal requirements, but additional posttreatment may be needed for discharge into waters with higher quality standards.

Swine wastewater differs from other livestock wastewater due to its higher concentrations of COD, ammonium, and phosphorus, as well as the presence of antibiotics, which can alter microbial activity and biofilm development (Massé et al., 2000; Zhao et al., 2020). Its higher organic load can lead to faster biochar saturation, reducing adsorption efficiency and increasing reliance on biodegradation. Additionally, excessive nitrogen may affect nitrification efficiency and microbial stability (Dong et al., 2023). These factors underscore the importance of optimizing loading rates and retention times in biochar filter systems to maintain effective treatment. Future studies should further explore microbial adaptations to different livestock wastewater compositions.

Conclusion

This study highlights the novel application of biochar-based UAF for treating pig farm wastewater, specifically using biochar from an invasive plant. System B, operating under higher OLR and HLR, achieved slightly better COD removal than system A, demonstrating that increased OLR can enhance biofilm growth, while elevated HLR may reduce efficiency due to shorter contact times. Both systems maintained effluent quality within regulatory standards, underscoring the importance of balancing OLR and HLR for cost-efficient performance. The research fills knowledge gaps by assessing *M. pigra* biochar performance under varying loading rates, highlighting its potential for resource-limited settings. The findings offer practical implications for small-scale farms and decentralized wastewater management. Biochar was produced at 600°C to optimize surface area and pollutant adsorption, which may increase energy costs compared with typical materials. However, using freely available locally sourced *M. pigra* helps offset production expenses. To enhance economic viability, further research on pyrolysis temperatures is needed to balance energy efficiency and treatment performance, along with studies on operational parameters and pollutant removal to improve wastewater reuse potential.

Authors' Contributions

All authors have read and agree with the published version of the article. Conceptualization: T.P.N. and X.C.N. Methodology: T.P.N. and X.C.N. Investigation: T.C.P.T., T.P.N., Q.V.L., N.-T.N., and N.-T.N. Validation: T.P.N. and X.C.N. Formal analysis: T.P.N., T.C.P.T., and T.T.N.N. Writing—original draft: T.P.N., X.C.N., T.P.N., Q.V.L., N.-T.N., N.-T.N., and X.C.N. Writing—review and editing: T.P.N. and X.C.N. Visualization: T.P.N., N.-T.N., and Q.V.L. Supervision: X.C.N. Funding acquisition: T.P.N.

Author Disclosure Statement

No competing financial interests exist.

Funding Information

This research was supported by Hue University—Quang Tri Branch (project code PH1-24).

Supplementary Material

Supplementary Figure S1
Supplementary Table S1

References

Almanassra IW, Mckay G, Kochkodan V, et al. A state of the art review on phosphate removal from water by biochars. Chem Eng J 2021;409:128211; doi: 10.1016/j.cej.2020.128211

APHA. Standard Methods for Examination of Water and Wastewater. APHA: Washington D.C.; 2017.

Bui VKH, Nguyen TP, Tran TCP, et al. Biochar-based fixed filter columns for water treatment: A comprehensive review. Sci Total Environ 2024;954:176199; doi: 10.1016/j.scitotenv.2024.176199

Chowdhury Z, Karim M, Ashraf M, et al. Influence of carbonization temperature on physicochemical properties of biochar derived from slow pyrolysis of Durian Wood (Durio zibethinus) Sawdust. Bioresources 2016;11(2):3356–3372; doi: 10.15376/biores.11.2.3356

Dai F, Zhuang Q, Huang G, et al. Infrared spectrum characteristics and quantification of OH Groups in Coal. ACS Omega 2023;8(19):17064–17076; doi: 10.1021/acsomega.3c01336

Dalahmeh SS. Capacity of biochar filters for wastewater treatment in onsite systems—technical report. SLU Report 2016;90.

Dalahmeh S, Ahrens L, Gros M, et al. Potential of biochar filters for onsite sewage treatment: Adsorption and biological degradation of pharmaceuticals in laboratory filters with active, inactive and no biofilm. Sci Total Environ 2018;612:192–201; doi: 10.1016/j.scitotenv.2017.08.178

Dalahmeh SS, Alziq N, Ahrens L. Potential of biochar filters for onsite wastewater treatment: Effects of active and inactive biofilms on adsorption of per- and polyfluoroalkyl substances in laboratory column experiments. Environ Pollut 2019a;247:155–164; doi: 10.1016/j.envpol.2019.01.032

Dalahmeh SS, Assayed A, Stenstrom Y. Combined vertical-horizontal flow biochar filter for onsite wastewater treatment-removal of organic matter, nitrogen and pathogens. Applied Sciences-Basel 2019b;9(24):5386; doi: 10.3390/app9245386

Dalahmeh SS, Pell M, Hylander LD, et al. Effects of changing hydraulic and organic loading rates on pollutant reduction in bark, charcoal and sand filters treating greywater. J Environ Manage 2014;132:338–345; doi: 10.1016/j.jenvman.2013.11.005

Delcourt N, Rébufa C, Dupuy N, et al. Infrared spectroscopy as a useful tool to predict land use depending on Mediterranean contrasted climate conditions: A case study on soils from olive-orchards and forests. Sci Total Environ 2019;686:179–190; doi: 10.1016/j.scitotenv.2019.05.240

Dissanayake PD, You S, Igalavithana AD, et al. Biochar-based adsorbents for carbon dioxide capture: A critical review. Renewable and Sustainable Energy Rev 2020;119:109582; doi: 10.1016/j.rser.2019.109582

Dobslaw D, Woiski C, Winkler F, et al. Prevention of clogging in a polyurethane foam packed biotrickling filter treating emissions of 2-butoxyethanol. J Cleaner Prod 2018;200:609–621; doi: 10.1016/j.jclepro.2018.07.248

Dong M, He L, Jiang M, et al. Biochar for the removal of emerging pollutants from aquatic systems: A review. Int J Environ Res Public Health 2023;20(3):1679; doi: 10.3390/ijerph20031679

Elnour A, Alghyamah A, Shaikh H, et al. Effect of pyrolysis temperature on biochar microstructural evolution, physicochemical characteristics, and its influence on biochar/polypropylene composites. Applied Sciences 2019;9(6):1149; doi: 10.3390/app9061149

Enaime G, Bacaoui A, Yaacoubi A, et al. Biochar for wastewater treatment—conversion technologies and applications. Applied Sciences 2020;10(10):3492; doi: 10.3390/app10103492

Escalante-Estrada V, Garzón-Zúñiga M, Valle-Cervantes S, et al. Swine wastewater treatment for small farms by a new anaerobic-aerobic biofiltration technology. Water Air Soil Pollut 2019;230(7):1–15; doi: 10.1007/s11270-019-4200-3

Fajar M, Sembiring E, Handajani M. The effect of filter media size and loading rate to filter performance of removing microplastics using rapid sand filter. J Eng Technol Sci 2022;54(5):220512; doi: 10.5614/j.eng.technol.sci.2022.54.5.12

Forbis-Stokes AA, Rocha-Melogno L, Deshusses MA. Nitrifying trickling filters and denitrifying bioreactors for nitrogen management of high-strength anaerobic digestion effluent. Chemosphere 2018;204:119–129; doi: 10.1016/j.chemosphere.2018.03.137

Gaur N, Dutta D, Jaiswal A, et al. Role and effect of persistent organic pollutants to our environment and wildlife. In: Persistent Organic Pollutants. IntechOpen: 2022; pp. 1–14.

Huong VTM. Research the efficiency of swine farm wastewater treatment treated by biogas by the model combination of constructed wetland and stabilisation pont in Thainguyen province. Journal of Military Science and Technology 2023:256–263; doi: 10.54939/1859-1043.j.mst.FEE.2023.256-263

Jayabalakrishnan RM, Kaviya S, Prasanthrajan M, et al. Efficiency of coconut adsorbent based filter system for textile dye industrial wastewater treatment. Int J Environ Analytical Chem 2024;104(19):7540–7552; doi: 10.1080/03067319.2023.2177955

Kaetzl K, Lübken M, Gehring T, et al. Efficient low-cost anaerobic treatment of wastewater using biochar and woodchip filters. Water 2018;10(7):818; doi: 10.3390/w10070818

Kaetzl K, Lübken M, Nettmann E, et al. Slow sand filtration of raw wastewater using biochar as an alternative filtration media. Sci Rep 2020;10(1):1229; doi: 10.1038/s41598-020-57981-0

Kaetzl K, Lübken M, Uzun G, et al. On-farm wastewater treatment using biochar from local agroresidues reduces pathogens from irrigation water for safer food production in developing countries. Sci Total Environ 2019;682:601–610; doi: 10.1016/j.scitotenv.2019.05.142

Kholoma E, Renman A, Renman G. Filter Media-Packed Bed Reactor Fortification with Biochar to Enhance Wastewater Quality. Applied Sciences 2020;10(3):790; doi: 10.3390/app10030790

Kim Y, Park Y, Han S, et al. Radiative and non-radiative decay pathways in carbon nanodots toward bioimaging and photodynamic therapy. Nanomaterials 2021;12(1):70.

Leng L, Xiong Q, Yang L, et al. An overview on engineering the surface area and porosity of biochar. Sci Total Environ 2021;763:144204; doi: 10.1016/j.scitotenv.2020.144204

Li H, Dong X, da Silva EB, et al. Mechanisms of metal sorption by biochars: Biochar characteristics and modifications. Chemosphere 2017;178:466–478; doi: 10.1016/j.chemosphere.2017.03.072

Li R, Wu Y, Lou X, et al. Porous biochar materials for sustainable water treatment: Synthesis, modification, and application. Water 2023;15(3):395; doi: 10.3390/w15030395

Loh ZZ, Zaidi NS, Syafiuddin A, et al. Shifting from conventional to organic filter media in wastewater biofiltration treatment: A review. Applied Sciences 2021;11(18):8650.

Lourinho G, Rodrigues L, Brito P. Recent advances on anaerobic digestion of swine wastewater. Int J Environ Sci Technol 2020;17(12):4917–4938; doi: 10.1007/s13762-020-02793-y

Majumder SD, Das A. Development of a full-scale cost effective mango peel biochar-sand filter based wastewater treatment chamber in Patharpratima in West Bengal. Ecological Engineering 2022;177:106565; doi: 10.1016/j.ecoleng.2022.106565

Marycz M. The use of Fungi in Biofiltration to Remove Hydrophobic Volatile Organic Compounds. Gdańsk University of Technology; 2023.

Massé DI, Lu D, Masse L, et al. Effect of antibiotics on psychrophilic anaerobic digestion of swine manure slurry in sequencing batch reactors. Bioresource Technology 2000;75(3):205–211; doi: 10.1016/S0960-8524(00)00046-8

Mesto E, Scordari F, Lacalamita M, et al. Tobelite and NH4+-rich muscovite single crystals from Ordovician Armorican sandstones (Brittany, France): Structure and crystal chemistry. American Mineralogist 2012;97(8–9):1460–1468; doi: 10.2138/am.2012.4023

Mohamed AYA, Tuohy P, Healy MG, et al. Effects of wastewater pre-treatment on clogging of an intermittent sand filter. Sci Total Environ 2023;876:162605; doi: 10.1016/j.scitotenv.2023.162605

MONRE. National Technical Regulation on Domestic Wastewater. Ministry of Natural Resources and Environment; 2025.

MONRE. National Technical Regulation on Livestock Wastewater. Ministry of Natural Resources and Environment; 2016.

Nguyen XC. Study on adsorption of methylene blue from aqueous solution by biochar derived from Mimosa pigra plant. VNU Journal of Science: Earth and Environmental Sciences 2021;37(2):43–54; doi: 10.25073/2588-1094/vnuees.4582

Nguyen THG, Ngo A, Huong LTT, et al. Recycling wastewater in intensive swine farms: Selected case studies in Vietnam. Journal-Faculty of Agriculture Kyushu University 2021;66:115–121; doi: 10.5109/4363559

Nguyen XC, Tran TCP, Hoang VH, et al. Combined biochar vertical flow and free-water surface constructed wetland system for dormitory sewage treatment and reuse. Sci Total Environ 2020;713:136404; doi: 10.1016/j.scitotenv.2019.136404

Perez-Mercado LF, Lalander C, Berger C, et al. Potential of biochar filters for onsite wastewater treatment: Effects of biochar type, physical properties and operating conditions. Water 2018;10(12):1835.

Phan CN, Strużyński A, Kowalik T, et al.; Faculty of Environmental Engineering and Land Surveying, University of Agriculture in Krakow. Environmental processes assessment of livestock wastewater treatment efficiency when using an anaerobic digester combined with a biological pond in Nam Anh, Nghe An, Vietnam. Acta Scientiarum Polonorum Formatio Circumiectus 2022;21(2):3–16; doi: 10.15576/ASP.FC/2022.21.2.3

Phuong Tran TC, Nguyen TP, Nguyen Nguyen TT, et al. Enhancement of phosphate adsorption by chemically modified biochars derived from Mimosa pigra invasive plant. Case Studies in Chemical and Environmental Engineering 2021;4:100117; doi: 10.1016/j.cscee.2021.100117

Pu Y, Tang J, Zeng T, et al. Pollutant removal and energy recovery from swine wastewater using anaerobic membrane bioreactor: A comparative study with up-flow anaerobic sludge blanket. Water 2022;14(15):2438; doi: 10.3390/w14152438

Rehman A, Ayub N, Naz I, et al. Effects of Hydraulic Retention Time (HRT) on the performance of a pilot-scale trickling filter system treating low-strength domestic wastewater. Pol J Environ Stud 2019;29(1):249–259; doi: 10.15244/pjoes/98998

Smith BC. The carbonyl group, part I: Introduction. Spectroscopy (Santa Monica) 2017;32:31–36.

Song Q, Kong F, Liu BF, et al. Biochar-based composites for removing chlorinated organic pollutants: Applications, mechanisms, and perspectives. Environ Sci Ecotechnol 2024;21:100420; doi: 10.1016/j.ese.2024.100420

Subratti A, Vidal JL, Lalgee LJ, et al. Preparation and characterization of biochar derived from the fruit seed of Cedrela odorata L and evaluation of its adsorption capacity with methylene blue. Sustainable Chemistry and Pharmacy 2021;21:100421; doi: 10.1016/j.scp.2021.100421

Terán R, De La Mora Orozco C, Acuña I, et al. Removing organic matter and nutrients from swine wastewater after anaerobic–aerobic treatment. Water 2017;9(10):726; doi: 10.3390/w9100726

Thai TTA, Nguyen TNB, Nguyen HC. Using aquatic plants as treatment for swine-breeding wastewater after biogas technology. Journal of Forestry Science and Technology 2022;14:089–097.

Tomczyk A, Sokołowska Z, Boguta P. Biochar physicochemical properties: Pyrolysis temperature and feedstock kind effects. Rev Environ Sci Biotechnol 2020;19(1):191–215.

Tran TCP, Nguyen TP, Nguyen TT, et al. Equilibrium single and co-adsorption of nutrients from aqueous solution onto aluminium-modified biochar. Case Studies in Chemical and Environmental Engineering 2022;5:100181; doi: 10.1016/j.cscee.2022.100181

Truong HB, Tran TCP, Nguyen TP, et al. Biochar-based phosphorus recovery from different waste streams: Sources, mechanisms, and performance. Sustainability 2023;15(21):15376; doi: 10.3390/su152115376

Wahyono T, Astuti D, Wiryawan K, et al. Fourier Transform Mid-Infrared (FTIR) spectroscopy to identify tannin compounds in the panicle of Sorghum Mutant Lines. IOP Conf Ser: Mater Sci Eng 2019;546(4):042045; doi: 10.1088/1757-899X/546/4/042045

Xiang W, Zhang X, Chen J, et al. Biochar technology in wastewater treatment: A critical review. Chemosphere 2020;252:126539; doi: 10.1016/j.chemosphere.2020.126539

Xin X, Liu SQ, Qin JW, et al. Performances of simultaneous enhanced removal of nitrogen and phosphorus via biological aerated filter with biochar as fillers under low dissolved oxygen for digested swine wastewater treatment. Bioprocess Biosyst Eng 2021;44(8):1741–1753; doi: 10.1007/s00449-021-02557-z

Yaashikaa PR, Kumar PS, Varjani S, et al. A critical review on the biochar production techniques, characterization, stability and applications for circular bioeconomy. Biotechnol Rep (Amst) 2020;28:e00570; doi: 10.1016/j.btre.2020.e00570

Zhang C, Ji Y, Li C, et al. The application of biochar for CO_2 Capture: Influence of biochar preparation and CO_2 capture reactors. Ind Eng Chem Res 2023;62(42):17168–17181; doi: 10.1021/acs.iecr.3c00445

Zhao B, Xie F, Zhang X, et al. Enhancing the nitrogen removal from swine wastewater digested liquid in a trickling biofilter with a soil layer. RSC Adv 2020;10(40):23782–23791; doi: 10.1039/D0RA03333B

Zhou L, Liang M, Zhang D, et al. Recent advances in swine wastewater treatment technologies for resource recovery: A comprehensive review. Sci Total Environ 2024;924:171557; doi: 10.1016/j.scitotenv.2024.171557